Latin American Journal of Solids and Structures
www.lajss.org

Explicit expression for effective moment of inertia of RC beams

Abstract

Deflection is an important design parameter for structures subjected to service load. This paper provides an explicit expression for effective moment of inertia considering cracking, for uniformly distributed loaded reinforced concrete (RC) beams. The proposed explicit expression can be used for rapid prediction of short-term deflection at service load. The explicit expression has been obtained from the trained neural network considering concrete cracking, tension stiffening and entire practical range of reinforcement. Three significant structural parameters have been identified that govern the change in effective moment of inertia and therefore deflection. These three parameters are chosen as inputs to train neural network. The training data sets for neural network are generated using finite element software ABAQUS. The explicit expression has been validated for a number of simply supported and continuous beams and it is shown that the predicted deflections have reasonable accuracy for practical purpose. A sensitivity analysis has been performed, which indicates substantial dependence of effective moment of inertia on the selected input parameters.

Keywords

Concrete cracking; deflection; finite element analysis; moment of inertia; neural network; reinforced concrete; tension stiffening.

K.A. Patel[a]
A. Bhardwaj[b]
S. Chaudhary[c]
A.K. Nagpal[d]

[a,b]Research Scholar, Civil Engg. Dept., IIT Delhi, New Delhi, India.
[c]Associate Professor, Civil Engg. Dept., MNIT Jaipur, Jaipur, India.
[d]Dogra Chair Professor, Civil Engg. Dept., IIT Delhi, New Delhi, India.

Corresponding author:
[a]iitd.kashyap@gmail.com
[b]ank.bhardwaj@gmail.com
[c]schaudhary.ce@mnit.ac.in
[d]aknagpal@civil.iitd.ac.in

http://dx.doi.org/10.1590/1679-78251272

Received 05.04.2014
In revised form 21.07.2014
Accepted 18.08.2014
Available online 13.10.2014

Nomenclatures

A_{st}, A_{sb}	area of top and bottom reinforcement, respectively
B, D	width and depth of beam
B_f, D_f	width and depth of flange
B_w, D_w	width and depth of web
E_c, E_s	modulus of elasticity of concrete and steel, respectively
I_e	effective moment of inertia
I_g, I_{cr}	moment of inertia of gross and fully cracked transformed cross section, respectively
I_j	j^{th} input parameter
L	length of beam

M_{cr}, M_e	minimum moment at which the cracking takes place at a cross-section in the beam and applied (elastic) moment, respectively
O_1	output parameter
$bias$	bias of hidden or output neuron
d_{EXP}, d_{FEM}, d_{NN}	mid-span deflection from experiments, FEM, and neural network/explicit expression, respectively
d_t, d_b	effective concrete cover at top and bottom. respectively
f_t	tensile strength of concrete
$f_c^{'}$	cylindrical compressive strength of concrete at 28 days
h_k	k^{th} hidden neuron
m	constant
q	number of input parameters
r	number of hidden neurons
w, n	uniformly distributed load and modular ratio, respectively
w_{cr}	minimum load at which the cracking takes place in the beam cracking
$w_{j,k}^{ih}$	weight of the link between I_j and h_k
$w_{k,1}^{ho}$	weight of the link between h_k and O_1
ε_{cr}, ε_u	cracking strain, and maximum tensile strain of concrete, respectively
ρ_t, ρ_c	percentage tension and compression reinforcement, respectively
Subscript	
j	input neuron number
k	hidden neuron number or function number
o	output neuron number
Superscript	
ho	connection between hidden and output layers
ih	connection between input and hidden layers

1 INTRODUCTION

Deflection is an important parameter to check the serviceability criteria of structure. The short term deflection is generally calculated using effective moment of inertia of entire span at service load. The equations for effective moment of inertia, available in literature, are mainly based on two approaches: (i) springs in parallel and (ii) springs in series (Kalkan, 2010). The stiffnesses of the uncracked and cracked portions are averaged in the springs in parallel approach (Branson, 1965; Al-Zaid et al., 1991; Al-Shaikh and Al-Zaid, 1993; SAA-AS 3600, 1994; TS 500, 2000; CSA-A23.3, 2004; ACI 318, 2005; AASHTO, 2005), whereas the flexibilities of the uncracked and cracked portions are averaged in the springs in series approach (Ghali, 1993; CEN Eurocode 2, 2004; Bischoff, 2005; Bischoff and Scanlon, 2007; Bischoff, 2007).

Considering parallel springs approach first, the following equation of effective moment of inertia I_e in terms of fully cracked and uncracked moment of inertia was originally proposed by Branson (1965) for simply supported beams as

$$I_e = \left(\frac{M_{cr}}{M_e}\right)^m I_g + \left[1 - \left(\frac{M_{cr}}{M_e}\right)^m\right] I_{cr} = I_{cr} + \left(\frac{M_{cr}}{M_e}\right)^m I_g - I_{cr} \leq I_g \tag{1}$$

where, M_{cr} = minimum moment at which the cracking takes place at a cross-section in the beam; M_e = applied (elastic) moment along the span; I_g = moment of inertia of the gross cross section; I_{cr} = moment of inertia of the fully cracked transformed cross section and m =constant.

Eq. (1) was derived empirically based on the experimental test results of simply supported rectangular reinforced concrete (RC) uniformly loaded beams with tension reinforcement, ρ_t = 1.65% and ratio of moment of inertia of the fully cracked transformed cross section and moment of inertia of the gross cross section, $I_{cr}/I_g = 0.45$ at maximum applied (elastic) moment equal to $2.5\,M_{cr}$ (Branson, 1965).

Eq. (1) has been adopted in many international standards and codes (SAA-AS 3600, 1994; TS 500, 2000; CSA-A23.3, 2004; ACI 318, 2005; AASHTO, 2005) to calculate I_e and therefore deflection, taking $m = 3$. Some researchers (Bischoff, 2005; Gilbert, 1999; Scanlon et al., 2001; Gilbert, 2006) found out that Eq. (1) with $m = 3$ calculates effective moment of inertia accurately in case of medium to high tension reinforcement($\rho_t >$ 1%), while it overestimates effective moment of inertia for low tension reinforcement ($\rho_t <$ 1%).

Al-Zaid et al. (1991) experimentally proved that the value of m in Eq. (1) depends on the loading configurations and suggested m = 2.8 (in Eq. (1)) for uniformly distributed load when $M_e > 1.5M_{cr}$. The value of m was found to change from about 3 to 4.3 for moderately-reinforced concrete beams (ρ_t = 1.2%, $I_{cr}/I_g = 0.34$) in the range of $M_{cr} < M_e < 1.5M_{cr}$. Al-Shaikh and Al-Zaid (1993) performed experiments on mid-span point loaded beams with varying reinforcement. The values of m was found to vary from about 1.8 to 2.5 for lightly reinforced beams (ρ_t = 0.8%, $I_{cr}/I_g = 0.22$) in the range of $1.5M_{cr} < M_e < 4M_{cr}$, while for the heavily reinforced beams (ρ_t = 2%, $I_{cr}/I_g = 0.44$), m varied in a range of 0.9 to 1.3. They also suggested $m = 3 - 0.8\rho_t$ incorporating reinforcement effect in Eq. (1) for point loaded beams. Al-Zaid et al. (1991); Al-Shaikh and Al-Zaid (1993) also proposed to calculate I_e based on cracked length incorporating reinforcement and loading effects respectively.

Next, consider the springs in series approach. The models based on this approach (Bischoff, 2005; Bischoff and Scanlon, 2007; Bischoff, 2007) take into account tension stiffening effect in concrete for calculating I_e. The deflections obtained by the expression proposed by Bischoff (2005) have been found in good agreement with experimental deflections for lightly reinforced beams ($\rho_t <$ 1%) (Gilbert, 2006; Bischoff and Scanlon, 2007).

Kalkan (2010) found out that the expressions given by Eq. (1) and Bischoff (2005) estimate deflections of moderately-reinforced to highly-reinforced concrete beams (ρ_t >1%) accurately on using the experimental value of cracking moment which, however, is difficult to obtain for each and every case.

It is observed from the review that no single approach or model is directly applicable for the entire range of practical reinforcement. Therefore, development of an approach for rapid estimation of the mid-span deflections in uniformly distributed loaded RC beams considering entire practical range of reinforcement at service load is desirable. The approach should be simple to use requiring a minimal computational effort but must give accuracy that is acceptable for practical applications. The application of neural network can be such an alternate approach. For generation of training data for neural networks, finite element technique may be used.

Nowadays, neural networks are being extensively applied in the field of structural engineering. Some of the recent applications of neural networks in the field of structural engineering include prediction of time effects in RC frames (Maru and Nagpal, 2004), prediction of damage detection in RC framed buildings after earthquake (Kanwar et al., 2007), structural health monitoring (Min et al., 2012; Kaloop and Kim, 2014), bending moment and deflection prediction in composite structures (Chaudhary et al., 2007, 2014; Pendharkar et al., 2007, 2010, 2011; Tadesse et al., 2012; Gupta et al., 2013), predicting the creep response of a rotating composite disc operating at elevated temperature (Gupta et al., 2007), optimum design of RC beams subjected to cost (Sarkar and Gupta, 2009), static model identification (Kim et al., 2009), response prediction of offshore floating structure (Uddin et al., 2012), prediction of deflection in high strength self-compacting concrete deep beams (Mohammadhassani et al., 2013a; 2013b) and prediction of energy absorption capability and mechanical properties of fiber reinforced self-compacting concrete containing nano-Silica particles (Tavakoli et al., 2014a; 2014b). These studies reveal the strength of neural networks in predicting the solutions of different structural engineering problems.

This paper presents an alternative approach for estimating effective moment of inertia which is neither spring in parallel nor spring in series approach. Neural network model is developed, at service load, for predicting effective moment of inertia (and deflection), in a RC beam considering entire practical range of tension and compression reinforcement, tension stiffening and flexural concrete cracking. The data sets for training, validating and testing are generated using finite element models. The finite element models have been developed in ABAQUS (2011) software and validated with the experimental results available in literature. Explicit expression has been obtained based on developed neural network model which can be used in design offices by practicing engineers. The proposed neural network/explicit expression has been validated for a number of simply supported and continuous RC beams. Sensitivity analysis has been performed to understand the influence of relevant parameters on effective moment of inertia.

2 FINITE ELEMENT MODEL AND ITS VALIDATION

The finite element model (FEM) has been developed using the ABAQUS (2011) software. The beam has been modelled using B21 elements (2-node linear Timoshenko beam element). Under service load, the stress-strain relationship of concrete is assumed to be linear in compression. Concrete has been considered as an elastic material in tension before cracking and softening behaviour is assumed after cracking (Figure 1). Further, at service load, the stress in reinforcement is assumed to be in the linear range. The steel reinforcement has been embedded into the concrete using "REBAR" option in which a perfect bond is considered between steel reinforcement and concrete. In order to consider cracking and tension stiffening, the smeared crack model has been used. Tension stiffening has been defined using post-failure stress-strain data proposed by Gilbert and Warner (1978). A high shear stiffness has been assumed to neglect the shear deformations.

The results of FEM have been compared with the experimental results (mid-span deflections of the beam under increasing uniformly distributed load, w, after the cracking of the concrete) reported by Al-Zaid et al. (1991) for a simply supported beam (VB) with 2.5 m clear span (effective span = 2.62 m) and cross-sectional dimensions $B \times D = 200 \times 200$ mm (Figure 2). The other properties considered are: cylindrical compressive strength of concrete at 28 days, $f_c^{'} = 38.2$

N/mm^2; modulus of elasticity of concrete, $E_c = 2.96\times10^4$ N/mm^2; modulus of elasticity of steel, $E_s = 2\times10^5$ N/mm^2; tensile strength of concrete, $f_t = 3.47$ N/mm^2; cracking moment, $M_{cr} = 5.2$ kNm; area of top reinforcement, $A_{st} = 78.54$ mm^2 and area of bottom reinforcement, $A_{sb} = 402.12$ mm^2. The effective concrete cover at top d_t and at bottom d_b have been taken as 30 mm and 33 mm respectively.

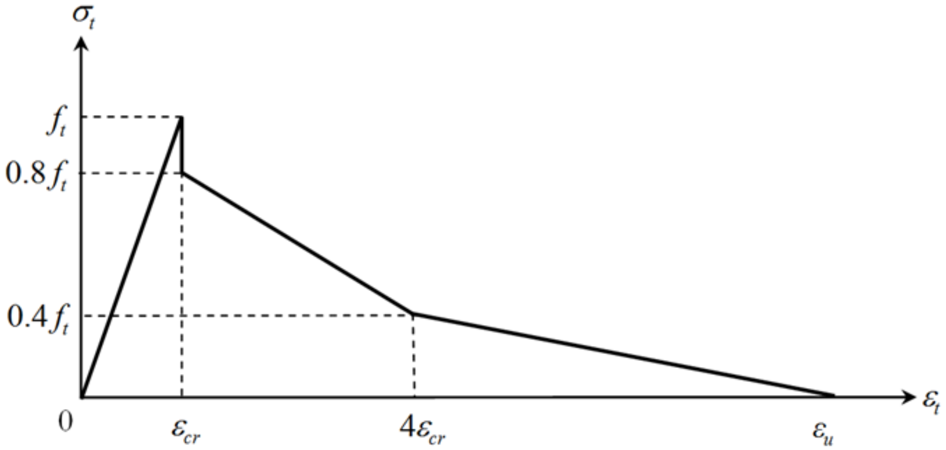

Figure 1: Tension stiffening model.

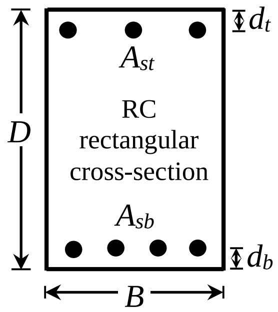

Figure 2: Rectangular cross-section.

In order to define the smeared crack model, the absolute value of the ratio of uniaxial tensile stress at failure to the uniaxial compressive stress at failure is taken as 0.09. The strain at cracking, ε_{cr} is taken as 0.00012 and in view of low/moderate tensile reinforcement, $A_{sb} = 402.12$ mm^2 (= 1.2%), the plastic strain is $\varepsilon_u - \varepsilon_{cr}$ taken as 0.0004. For convergence, about 16 elements are required when cracking is considered (Patel et al., 2014). Results from the developed FEM and experiments are compared in Figure 3. Close agreement is observed between the results from FEM and experiments.

Next, the results have been compared with experimental results reported by Washa and Fluck (1952) for four sets of rectangular cross-sectional (Figure 2) simply supported beams: A1,A4; B1,B4; C1,C4; D1,D4 subjected to uniformly distributed loads at service load. Two beams in a set are identical. The cross-sectional properties, material properties, span lengths and uniform distributed loads of all four beams have been given in Table 1. Additionally, E_s has been assumed as 2×10^5 N/mm^2. E_c and f_t are taken in accordance with ACI 318 (2005). The mid-span deflections obtained from the FEM d_{FEM} are in close agreement with the reported experimental deflections d_{EXP} as shown in Table 1. The finite element models can therefore be used for generation of data sets.

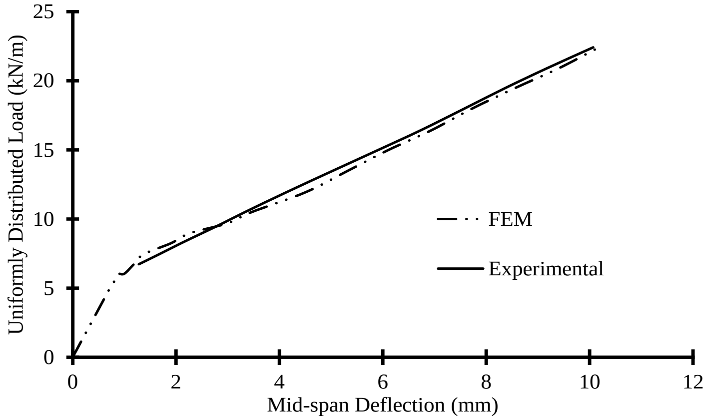

Figure 3: Comparison of mid-span deflections of beam VB.

Beams	Properties								Mid-span deflections	
	B (mm)	D (mm)	M (kNm)	w (kN/m)	f_c' (N/mm^2)	L (mm)	$d_t=d_b$ (mm)	$A_{st}=A_{sb}$ (mm^2)	d_{EXP} (mm)	d_{FEM} (mm)
A1-A4	203	305	25.65	5.52	28.1	6096	48	852	13.50	13.27
B1-B4	152	203	7.25	1.56	23.6	6096	46	400	23.40	23.38
C1-C4	305	127	6.01	1.20	22.7	6340	25	516	40.10	39.75
D1-D4	305	127	6.07	3.35	24.3	3810	25	516	12.00	13.17

Table 1: Properties of simply supported beams with rectangular cross-sections, considered for validation of FE model.

3 SAMPLING POINTS AND DATA SETS

For development of neural network, significant parameters need to be identified. Eq. (1) shows that I_e/I_g explicitly depends on I_{cr}/I_g and M_{cr}/M_a. It is assumed that I_e/I_g depends on ρ_t and ρ_c (percentage compression reinforcement) also. The value of ρ_c however depends on ρ_t and ranges from 0.0 to $\rho_t(n-1)/n$, where, n = modular ratio. The value of I_{cr}/I_g in turn also depends on the combinations of ρ_t and ρ_c. Consider a typical beam cross-section as shown in Figure 2 (B = 300 mm; D = 700 mm; $E_c = 2.73\times10^4\ N/mm^2$; $E_s = 2.00\times10^5$ N/mm^2; d_t = 30 mm and d_b = 33 mm). For this beam, the variations of ρ_c and I_{cr}/I_g with ρ_t are shown in Figure 4. The parameter M_{cr}/M_a depends on the load and moment only.

Taking the above observations into account, ρ_t is also considered as an input parameter alongwith I_{cr}/I_g and M_{cr}/M_e. The sampling points of the parameters considered for data generation are shown in Table 2. It may be noted that the combinations of sampling points take into account the different values of the ρ_c (fourth and left out parameter), corresponding to each value of ρ_t. Considering the equation $d_{FEM} = 5wL^4 / 384E_c I_e$, the output parameter I_e/I_g is obtained as $5wL^4 / 384E_c d_{FEM} I_g$.

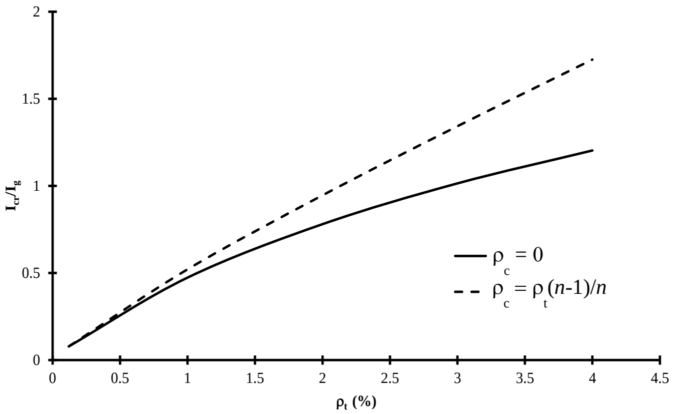

Figure 4: Variation of ρ_c and I_{cr}/I_g with ρ_t.

Input Parameters	Sampling points								
ρ_t	0.12	0.15	0.25	0.45	0.75	1.00	2.00	3.00	4.00
I_{cr}/I_g	0.0783	0.0963	0.1525	0.2550	0.3785 0.4085	0.4734 0.4993 0.4734	0.7802 0.8733 0.7802	1.0143 1.1461 1.2538 1.3425	1.2032 1.3684 1.5073 1.6249 1.7253
M_{cr}/M_e	As per increment in FE analysis								

Table 2: Input parameters and sampling points.

4 TRAINING OF NEURAL NETWORK

Neural network has been developed for the prediction of effective moment of inertia in RC beams. The neural network chosen is a set of multilayered feed-forward networks with neurons in all the layers fully connected in the feed forward manner (Figure 5). The training is carried out using the MATLAB Neural Network toolbox (2009). Sigmoid function (logsig) is used as an activation function and the Levenberg-Marquardt back propagation learning algorithm (trainlm) is used for training. The back propagation algorithm has been used successfully for many structural engineering applications (Maru and Nagpal, 2004; Kanwar et al., 2007; Gupta et al., 2007; Pendharkar et al., 2007; 2010; 2011; Chaudhary et al., 2007; 2014; Sarkar and Gupta, 2009; Gupta and Sarkar, 2009; Min et al., 2012; Tadesse et al., 2012; Mohammadhassani et al., 2013a; Gupta et al., 2013) and is considered as one of the efficient algorithms in engineering applications (Hsu et al., 1993). One hidden layer is chosen and the number of neurons in the layer is decided in the learning process by trial and error.

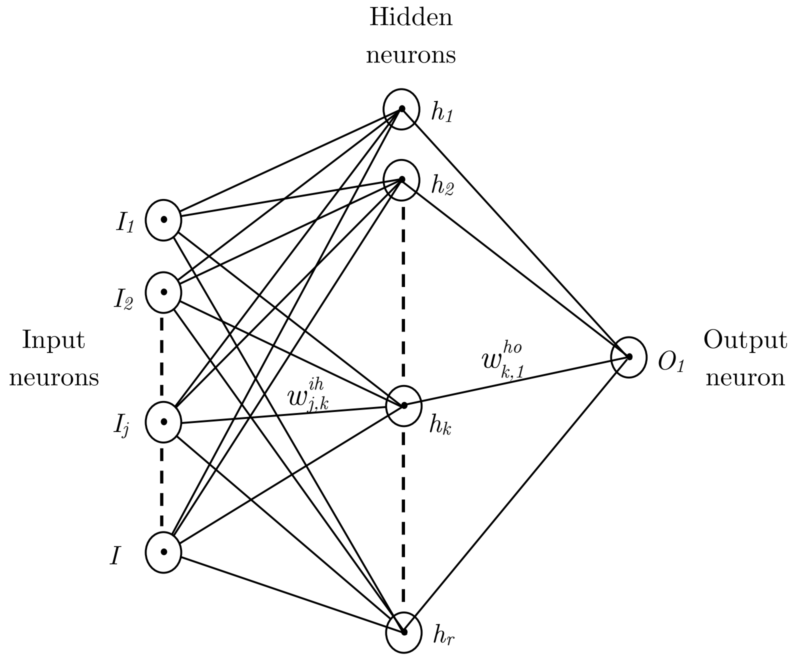

Figure 5: Configuration of a typical neural network.

Different combinations of sampling points of the input parameters and the resulting values of the output parameters are considered in order to train the neural network. Each such combination of the input parameters and the resulting output parameters comprises a data set. The total number of data sets considered for the training, validating and testing of the network are 3444.

Normalisation factors are applied to input and output parameter to bring and well distribute them in the range. No bias is applied to the input and output parameters. Normalisation factors of 4, 2, 7 and 3 are applied to input parameters ρ_t, I_{cr}/I_g, M_{cr}/M_e and output parameter I_e/I_g respectively.

70% data sets are used for training and the remaining data sets are divided equally in the validating and testing sets. For the training, several trials are carried out with different numbers of neurons in the hidden layer starting with a small number of neurons in the hidden layer and progressively increasing it, and checking the mean square errors (MSE) for the training, validating and testing. The number of neurons in the hidden layer is decided on the basis of the least mean square errors (MSE) for the training as well as validating and testing. Care is taken that the mean square error for test results should not increase with the number of neurons in hidden layer or epochs (overtraining). The final configuration (number of input parameters - number of neurons in the hidden layer - number of output parameters) of NN is 3-6-1. The responses of proposed neural network model to predict effective moment of inertia for training, validating, and testing are shown in Figures 6(a)-(c) respectively. The proposed neural network model achieved good performance as the testing data points are mostly on equity line (Figure 6(c)). The statistical parameters i.e. mean square error (MSE), root mean square error (RMSE), mean absolute percentage error (MAPE), average absolute deviation (AAD), correlation coefficient (R^2) and coefficient of variation (COV) (Sozen et al., 2004; Azmathullah et al., 2005) of training, validating and testing data sets are shown in Table 3. All the parameters indicate a good agreement.

Statistical	Data sets		
parameters	Training	Validating	Testing
MSE	0.00005	0.00006	0.00006
RMSE	0.00735	0.00742	0.00748
MAPE	1.99790	2.00716	2.05474
AAD	1.75733	1.78257	1.78176
R^2	0.99819	0.99822	0.99815
COV	2.31244	2.33217	2.3433

Table 3: Statistical parameters of neural network.

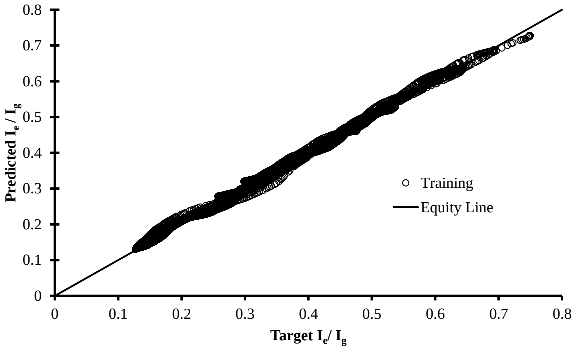

(a)

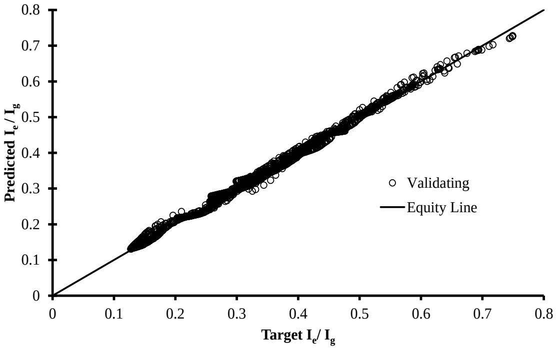

(b)

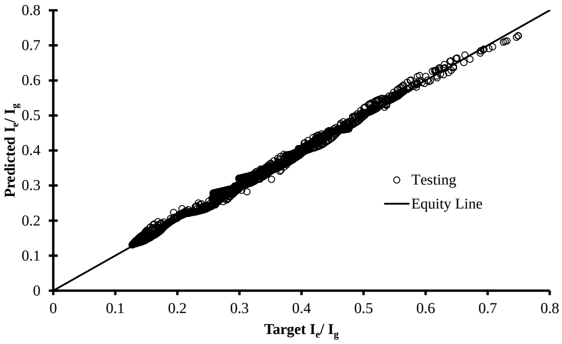

(c)

Figure 6: Response of neural network model in predicting I_e/I_g : (a) training; (b) validating; and (c) testing.

5 EXPLICIT EXPRESSION FOR PREDICTION OF EFFECTIVE MOMENT OF INERTIA

For the ease of practicing engineers and users, simplified explicit expression can be developed for the prediction of effective moment of inertia. The explicit expression requires the values of inputs, weights of the links between the neurons in different layers, and biases of output neurons (Tadesse et al., 2012; Gupta et al., 2013).

As stated earlier, the sigmoid function (logsig) has been used as the activation function. The output O_1 (Figure 5) may therefore be obtained as below (Tadesse et al., 2012; Gupta et al., 2013):

$$O_1 = \frac{1}{1 + e^{-\left(bias_{\mathrm{o}} + \sum_{k=1}^{r} \frac{w^{ho}_{\mathrm{k},1}}{1+e^{-H_k}}\right)}} \tag{2}$$

$$H_{\mathrm{k}} = \sum_{j=1}^{q} w^{\mathrm{ih}}_{\mathrm{j,k}} \times I_{\mathrm{j}} + bias_{\mathrm{k}} \tag{3}$$

where, q and r are the number of input parameters and the number of hidden neurons respectively; $bias_{\mathrm{k}}$ and $bias_{\mathrm{o}}$ are the bias of k^{th} hidden neuron (h_{k}) and the bias of output neuron respectively; $w^{\mathrm{ih}}_{\mathrm{j,k}}$ and $w^{\mathrm{ho}}_{\mathrm{k,1}}$ are the weight of the link between I_{j} and h_{k} and the weight of the link between h_{k} and O_1 respectively. The weights of the links and biases of the output neurons for NN are listed in Table 4.

Connection	Weight/ Bias	Number of the hidden layer neuron (k)					
		1	2	3	4	5	6
Input to Hidden	$w^{ih}_{1,k}$	-0.1978	4.3806	2.8322	3.0191	10.1889	-3.7310
	$w^{ih}_{2,k}$	1.2333	-22.0048	-4.1654	-4.3927	-15.7592	5.4520
	$w^{ih}_{3,k}$	0.0011	-0.1823	9.4775	9.7598	5.0682	-0.0189
	$bias_k$	-0.0386	6.2396	-6.7756	-7.1914	-3.2443	-2.9660
Hidden to Output	$w^{ho}_{k,1}$	8.7116	-0.3754	11.6985	-10.7167	0.6177	22.9397

Table 4: Weight values and biases of neural network.

The value of I_e/I_g is equal to de-normalized output O_1. The effective moment of inertia I_e may be obtained from Eq. (2) by putting the values of $w^{ho}_{k,1}$ from Table 4 as

$$I_e = \frac{3 \times I_g}{1 + e^{-\left(-7.4688 + \frac{8.7116}{1+e^{-H_1}} - \frac{0.3754}{1+e^{-H_2}} + \frac{11.6985}{1+e^{-H_3}} - \frac{10.7167}{1+e^{-H_4}} + \frac{0.6177}{1+e^{-H_5}} + \frac{22.9397}{1+e^{-H_6}}\right)}} \tag{4}$$

where, H_1, H_2, H_3, H_4, H_5 and H_6 may be obtained from Eqs. (5)-(10) by using the weights and biases (Table 4) as

$$H_1 = -0.1978 \times \rho_t + 1.2333 \times I_{cr}/I_g + 0.0011 \times M_{cr}/M_e - 0.0386 \tag{5}$$

$$H_2 = 4.3806 \times \rho_t - 22.0048 \times I_{cr}/I_g - 0.1823 \times M_{cr}/M_e + 6.2396 \tag{6}$$

$$H_3 = 2.8322 \times \rho_t - 4.1654 \times I_{cr}/I_g + 9.4775 \times M_{cr}/M_e - 6.7756 \tag{7}$$

$$H_4 = 3.0191 \times \rho_t - 4.3927 \times I_{cr}/I_g + 9.7578 \times M_{cr}/M_e - 7.1914 \tag{8}$$

$$H_5 = 10.1889 \times \rho_t - 15.7592 \times I_{cr}/I_g + 5.0682 \times M_{cr}/M_e - 3.2443 \tag{9}$$

$$H_6 = -3.7310 \times \rho_t + 5.4520 \times I_{cr}/I_g - 0.0189 \times M_{cr}/M_e - 2.9660 \tag{10}$$

6 VALIDATION OF NEURAL NETWORK/ EXPLICIT EXPRESSION

The developed neural network/explicit expression is validated for a number of simply supported and continuous beams with a wide variation of input parameters. The results (mid-span deflections), obtained from the proposed neural network/explicit expression are compared with the experimental results for simply supported beams available in literature and with the FEM results for continuous beams.

6.1 Simply supported beams

First, the results have been compared with experimental results reported by Washa and Fluck (1952) for sets of simply supported beams with rectangular cross-section (Figure 2): A2,A5; B2,B5; C2,C5; D2,D5 subjected to uniformly distributed loads, and designated, here, as VB1-VB4, respectively. Two beams in a set are identical. The details of the beams are given in Table 5. Additionally, E_s is assumed as 2.05×10^5 N/mm^2. E_c and f_t are taken in accordance with ACI 318 (2005). The mid-span deflections obtained from the proposed explicit expression d_{NN} are shown in Table 5 along with the reported experimental mid-span deflections d_{EXP}. The values obtained from the proposed explicit expression are in reasonable agreement with the reported experimental values of mid-span deflections.

Beams	Properties									Mid-span deflections	
	B (mm)	D (mm)	M (kNm)	w (kN/m)	f_c' (N/mm^2)	L (mm)	$d_t = d_b$ (mm)	A_{st} (mm^2)	A_{sb} (mm^2)	d_{EXP} (mm)	d_{NN} (mm)
VB1 (A2,A5)	203	305	25.65	5.52	28.1	6096	48	400	852	15.80	13.55
VB2 (B2,B5)	152	203	7.25	1.56	23.6	6096	46	200	400	24.90	24.41
VB3 (C2,C5)	305	127	6.01	1.20	22.7	6340	25	258	516	43.40	39.48
VB4 (D2,D5)	305	127	6.07	3.35	24.3	3810	25	258	516	14.20	14.24

Table 5: Properties of simply supported beams with rectangular cross-sections, considered for validation of the explicit expression.

Next, the results have been compared with experimental results reported by Yu and Winter (1960) for simply supported beams with T cross-section (Figure 7): A-1; B-1; C-1; D-1; E-1; F-1 subjected to uniformly distributed loads, and designated, here, as VB5-VB10, respectively. The cross-sectional and material properties of the beams are given in Table 6. The mid-span deflections obtained from the proposed explicit expression d_{NN} are shown in Table 6 along with the reported experimental mid-span deflections d_{EXP}. Again, the values obtained from the proposed explicit expression are in reasonable agreement with the reported experimental values of mid-span deflections.

The results (mid-span deflections) obtained from the proposed neural network/explicit expression need to be compared with the finite element results for lightly reinforced simply supported beams $\rho_t \leq 1\%$ also. Consider a 2.625 m long simply supported beam VB11 with rectangular cross-section (Figure 2) subjected to uniformly distributed load. The other properties are: $B =$ 200 mm; $D =$ 500 mm; $f_c' =$ 27.9 N/mm^2; $E_s =$ 2.05×10^5 N/mm^2; $A_{st} =$ 400 mm^2; $A_{sb} =$

700 mm^2; $d_t = d_b =$ 35 mm. E_c and f_t are taken in accordance with ACI 318 (2005). Mid-span deflections, for beam VB11 are obtained from the proposed explicit expression, FEM and ACI 318 (2005) for varying magnitude of uniformly distributed loads, w and shown in Figure 8. The mid-span deflections obtained from the proposed explicit expression and FEM are close for the range of the load considered. The difference between FEM and proposed explicit expression is 2.91% as compared to 16.81% difference between FEM and ACI 318 (2005) at $4w_{cr}$,(w_{cr} = cracking uniformly distributed load).

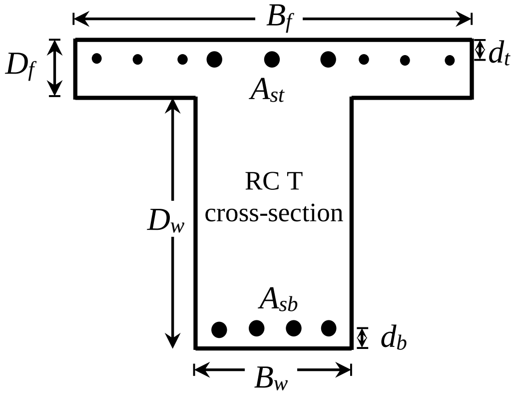

Figure 7: T cross-section.

Parameters	Properties of beams					
	VB5 (A-1)	VB6 (B-1)	VB7 (C-1)	VB8 (D-1)	VB9 (E-1)	VB10 (F-1)
B_f (mm)	304.87	304.87	304.87	609.74	304.87	304.87
D_f (mm)	63.52	63.52	63.52	63.52	63.52	50.81
B_w (mm)	152.44	152.44	152.44	152.44	152.44	152.44
D_w (mm)	241.36	241.36	241.36	241.36	241.36	152.44
d_t (mm)	-	39.63	39.63	-	-	-
d_b (mm)	45.98	45.98	45.98	58.94	55.64	45.98
A_{st} (mm^2)	-	200.09	400.19	-	-	-
A_{sb} (mm^2)	400.19	400.19	400.19	774.56	400.19	400.19
f'_c (N/mm^2)	25.37	26.77	24.27	25.37	29.36	29.36
E_c (N/mm^2)	2.53×10^4	2.60×10^4	2.47×10^4	2.53×10^4	2.72×10^4	2.72×10^4
E_s (N/mm^2)	2.05×10^5	2.05×10^5	2.05×10^5	2.05×10^5	2.05×10^5	2.05×10^5
w (N/mm)	6.42	6.44	6.41	11.73	12.29	3.79
f_t (N/mm^2)	2.78	2.66	2.73	2.78	3.06	3.06
L (mm)	6098	6098	6098	6098	4268	6098
Mid-span deflections						
d_{EXP} (mm)	34.04	31.50	30.23	32.23	12.96	55.89
d_{NN} (mm)	30.21	29.88	30.00	32.72	14.66	51.83

Table 6: Properties of simply supported beams with T cross-sections, considered for validation of the explicit expression.

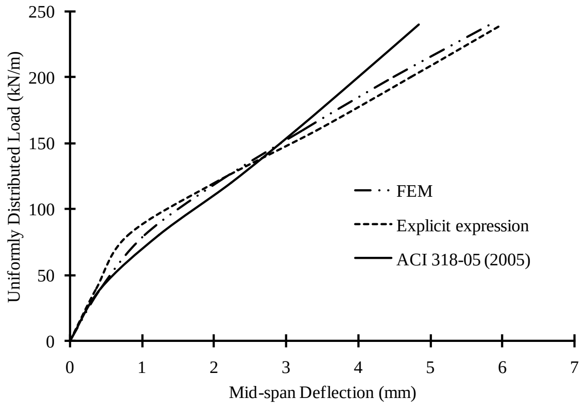

Figure 8: Comparison of mid-span deflections of beam VB11.

Consider another simply supported beam VB12 subjected to uniformly distributed load with the same cross-sectional (Figure 2) and material properties as that of beam VB11 except A_{sb}. The value of A_{sb} is now assumed as 900 mm^2. The close agreement is observed between the mid-span deflections obtained from the proposed explicit expression, FEM and ACI 318 (2005) as shown in Figure 9.

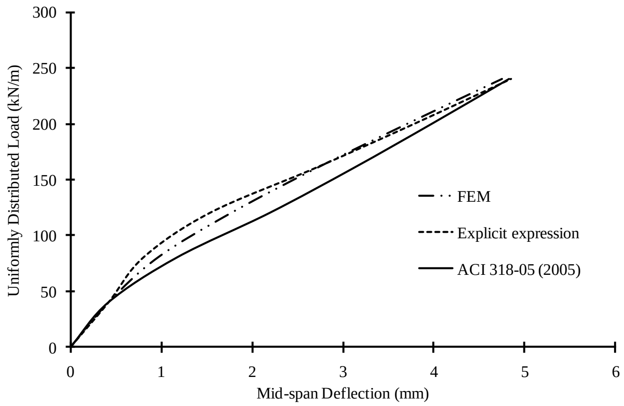

Figure 9: Comparison of mid-span deflections of beam VB12.

6.2 Continuous beams

In order to validate the proposed explicit expression for a continuous beam, results from the explicit expression are also compared with FEM and ACI 318 (2005) results for a 12.2 m two equal span uniformly distributed loaded continuous beam (VB13) with rectangular cross-section (Figure 2). The other properties are: $B =$ 152.4 mm; $D =$ 203.2 mm; $f_c^{'} =$ 24.1 N/mm^2; $E_s =$ 2.07x10^5 N/mm^2; $A_{st} = A_{sb} =$ 112 mm^2; $d_t = d_b =$ 25 mm. E_c and f_t are taken in accordance with ACI 318 (2005).

The mid-span deflections obtained from the proposed explicit expression and FEM are close for the range of the load considered (Figure 10). The difference between FEM and proposed explicit expression is 5.34% as compared to 28.25% difference between FEM and ACI 318 (2005) at $5w_{cr}$.

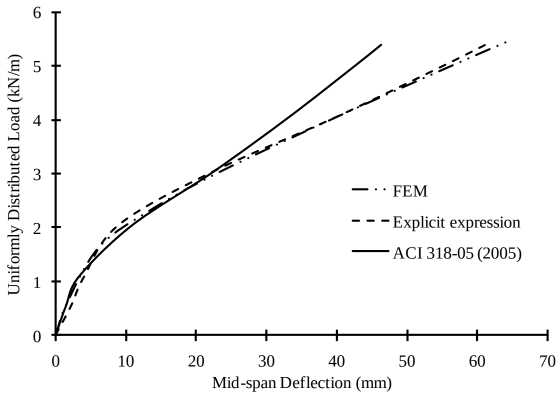

Figure 10: Comparison of mid-span deflections of beam VB13.

Similarly, another 12.2 m two equal span continuous beam VB14 with rectangular cross-section (Figure 2) subjected to uniformly distributed load has been considered. The cross-sectional and material properties are taken same as that of beam VB13 and only A_{sb} and A_{st} are increased to 200 mm^2. The close agreement is observed between the mid-span deflections obtained from the proposed explicit expression, FEM and ACI 318 (2005) as shown in Figure 11.

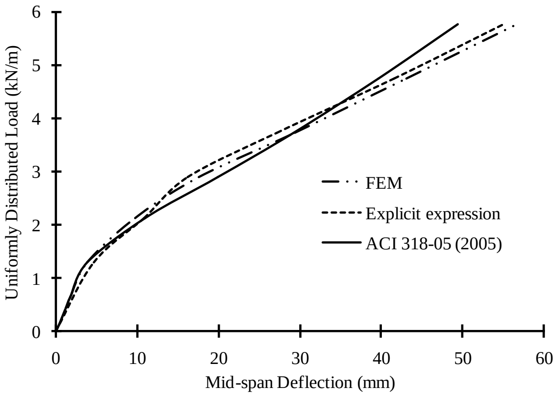

Figure 11: Comparison of mid-span deflections of beam VB14.

7 SENSITIVITY ANALYSIS

The proposed explicit expression shows satisfactory performance on validation with experimental results available in literature and FEM results. A sensitivity analysis is carried out next to capture the influence of individual input parameters on output parameter using the proposed explicit expression. The effect of input parameters ρ_t, I_{cr}/I_g, M_{cr}/M_e along with additional parameters ρ_c, n on output parameter I_e/I_g is studied. Only one parameter (the parameter under consideration) is varied at a time, keeping the other parameters constant.

7.1 Effect of ρ_t

As stated earlier, ρ_t has been considered as the input parameter in the present study. Figure 12 shows the variation of I_e/I_g with respect to ρ_t for various values of I_{cr}/I_g, keeping the value of

M_{cr}/M_e constant as 0.5. Rich influence of ρ_t on I_e/I_g is seen in Figure 12. Though, the effect is significant for all values of ρ_t, the effect of lower values of ρ_t is more significant in case of higher I_{cr}/I_g.

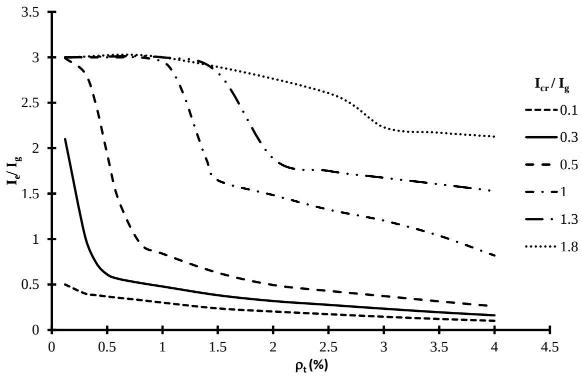

Figure 12: Variation of I_e/I_g with respect to ρ_t.

7.2 Effect of I_{cr}/I_g

The variation of I_e/I_g with respect to I_{cr}/I_g for various values of ρ_t is shown in Figure 13. The value of M_{cr}/M_e is kept constant as 0.5. The effect is significant only for lower values of I_{cr}/I_g in case of low ρ_t. However, the effect extends of the range considered for I_{cr}/I_g in case of higher values of ρ_t. The effect of I_{cr}/I_g is significant for all values of ρ_t.

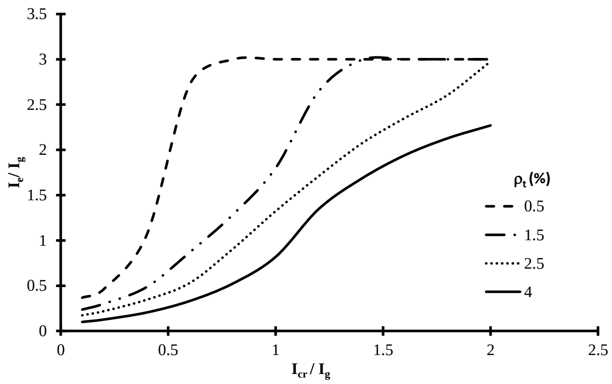

Figure 13: Variation of I_e/I_g with respect to I_{cr}/I_g.

7.3 Effect of M_{cr}/M_e

As stated earlier, M_{cr}/M_e has been considered as the input parameter affecting I_e/I_g. The variation of I_e/I_g with respect to M_{cr}/M_e for different values of ρ_t is shown in Figure 14(a). The value of I_{cr}/I_g is kept constant as 0.5. Similarly, Figure 14(b) shows the variation of the ratio I_e/I_g with respect to M_{cr}/M_e for different values of I_{cr}/I_g. The value of ρ_t is kept constant as 1.5. As expected, the effect of M_{cr}/M_e is significant during cracking $M_{cr}/M_e < 1$ and the value of I_e/I_g increases with increase in value of M_{cr}/M_e up to 1.00. The effect is more for higher value of ρ_t.

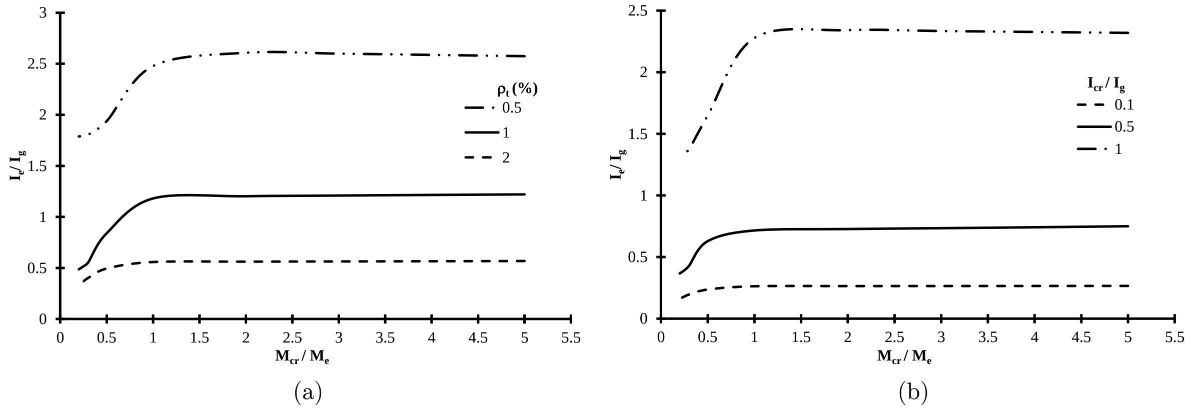

Figure 14: Variation of I_e/I_g with respect to M_{cr}/M_e for different (a) ρ_t values, and (b) I_{cr}/I_g values.

7.4 Effect of ρ_c

Figure 15 shows the variation of I_e/I_g with respect to ρ_c for different values of ρ_t. The value of M_{cr}/M_e is kept constant as 0.5. The value of I_e/I_g is found to increase with the increase in value of ρ_c. A significant variation is observed in case of higher value of ρ_t.

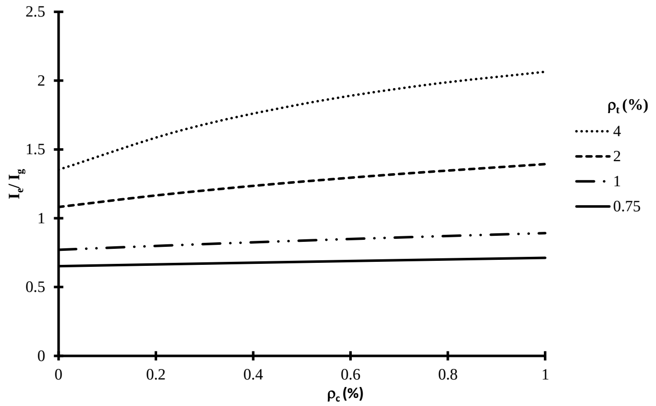

Figure 15: Variation of I_e/I_g with respect to ρ_c.

7.5 Effect of n

The variation of I_e/I_g with respect to n for different values of ρ_t is shown in Figures 16(a)-(b) for $\rho_c = 0$ and $\rho_c = \rho_t(n-1)/n$ respectively. The value of M_{cr}/M_e is kept constant as 0.5. The nature of plot changes from concave to convex with increase in ρ_t.

8 CONCLUSIONS

An explicit expression has been proposed for the prediction of effective moment of inertia (and deflection) considering concrete cracking, tension stiffening and entire practical range of reinforcement at service load. A set of three parameters (ρ_t, I_{cr}/I_g, M_{cr}/M_e) has been identified that govern the change in I_e/I_g and therefore deflection. Using the sampling points of these parameters and the validated FEM, the data sets have been generated for training, validating and testing of neural network. The explicit expression has been developed from the trained neural network. The proposed explicit expression has been validated for a number of simply supported and continuous beams and it is found that the predicted deflections have reasonable accuracy for practical purpose. Sensitivity analysis has been carried out to capture the influence of individual input parameters on output parameter. The effect of the input parameters ρ_t , I_{cr}/I_g , M_{cr}/M_e on output parameter I_e/I_g is studied using the proposed explicit expression . The lower values of ρ_t are found to have more significant effect on I_e/I_g . The effect of M_{cr}/M_e is found to be significant during cracking $M_{cr}/M_e < 1$ and the value of I_e/I_g is found to increase up to 10.0 with increase in value of M_{cr}/M_e . The effect of ρ_c and n is found to be less significant and can be incorporated through I_{cr}/I_g .

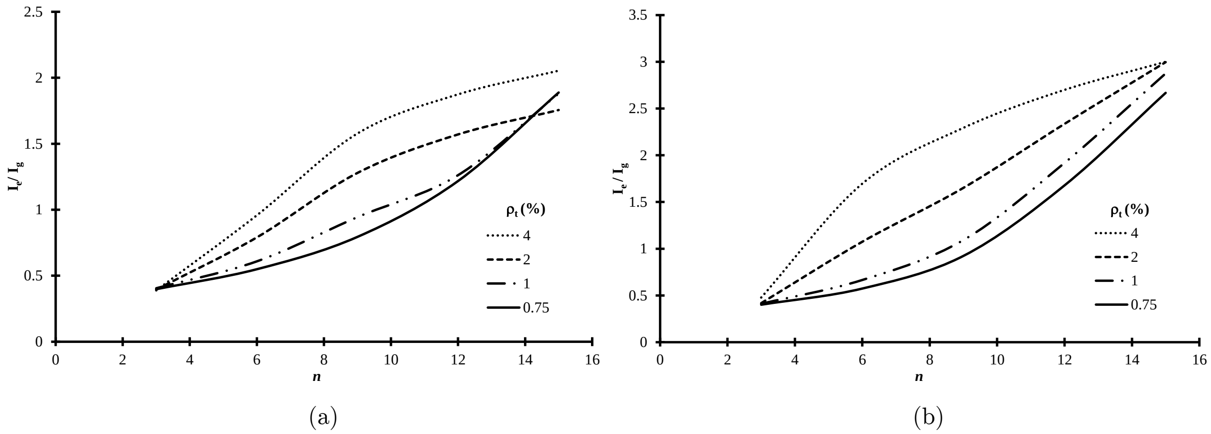

Figure 16: Variation of I_e/I_g with respect to n for (a) $\rho_c = 0$ and (b) $\rho_c = \rho_t(n-1)/n$.

The methodology presented herein can be further developed for beams with point loads. The effect of shear deformation may be incorporated in future studies by considering span to depth ratio of beam as an input parameter. Similarly, age of loading and characteristic compressive strength of concrete can also be considered as input parameters to account for shrinkage cracking in future studies.

References

ABAQUS 6.11, Standard user's manuals, USA, 2011.

Al-Shaikh, A.H., Al-Zaid, R.Z., (1993). Effect of reinforcement ratio on the effective moment of inertia of reinforced concrete beams. ACI Structural Journal 90(2): 144-149.

Al-Zaid, R.Z., Al-Shaikh, A.H., Abu-Hussein, M.M., (1991). Effect of loading type on the effective moment of inertia of reinforced concrete beams. ACI Structural Journal 88(2): 184-190.

American Association of State Highway and Transportation Officials (AASHTO), (2005). AASHTO LRFD bridge design specifications (SI units), USA.

American Concrete Institute (ACI) 318, (2005). Building code requirements for structural concrete (ACI 318-05) and commentary (ACI 318R-05), USA.

Azmathullah, M.C., Deo, M.C., Deolalikar, P.B., (2005). Neural networks for estimation of scour downstream of a ski-jump bucket. Journal of Hydraulic Engineering ASCE 131(10): 898-908.

Bischoff, P.H., (2005). Reevaluation of deflection prediction for concrete beams reinforced with steel and fiber reinforced polymer bars. Journal of Structural Engineering ASCE 131(5): 752-762.

Bischoff, P.H., (2007). Rational model for calculating deflection of reinforced concrete beams and slabs. Canadian Journal of Civil Engineering 34(8): 992-1002.

Bischoff, P.H., Scanlon, A., (2007). Effective moment of inertia for calculating deflections of concrete members containing steel reinforcement and fiber-reinforced polymer reinforcement. ACI Structural Journal 104(1): 68-75.

Branson, D.E., (1965). Instantaneous and time-dependent deflections of simple and continuous reinforced concrete beams, HPR Report No.7(1), Alabama Highway Department, Bureau of Public Roads, Alabama: 1-78.

Canadian Standards Association (CSA) A23.3, (2004). Design of concrete structures, Canada.

Chaudhary, S., Pendharkar, U., Nagpal, A.K., (2007). Bending moment prediction for continuous composite beams by neural networks. Advances in Structural Engineering 10(4): 439-454.

Chaudhary, S., Pendharkar, U., Patel, K.A., Nagpal, A.K., (2014). Neural networks for deflections in continuous composite beams considering concrete cracking. Iranian Journal of Science and Technology: Transactions of Civil Engineering 38($C1^+$): 205-221.

European Committee for Standardization (CEN) Eurocode 2 BS EN 1992-1-1, (2004). Design of concrete structures-Part 1-1: General rules and rules for buildings, Belgium.

Ghali, A., (1993). Deflection of reinforced concrete members: A critical review. ACI Structural Journal 90(4): 364-373.

Gilbert, R.I., (1999). Deflection calculation for reinforced concrete Structures- Why we sometimes get it wrong. ACI Structural Journal 96(6): 1027-1033.

Gilbert, R.I., (2006). Discussion of ‘Reevaluation of deflection prediction for concrete beams reinforced with steel and fiber reinforced polymer bars’ by P.H. Bischoff. Journal of Structural Engineering ASCE 132(8): 1328-1330.

Gilbert, R.I., Warner, R.F., (1978). Tension stiffening in reinforced concrete slabs. Journal of Structural Division ASCE 104(12): 1885-1900.

Gupta, M.K., Sarkar, K., (2009).Modeling of section forces in a continuous beam using artificial neural. Journal of Structural Engineering SERC 35(6): 416-422.

Gupta, R.K., Patel, K.A., Chaudhary, S., Nagpal, A. K., (2013). Closed form solution for deflection of flexible composite bridges. Procedia Engineering 51: 75-83.

Gupta, V.K., Kwatra, N., Ray, S., (2007). Artificial neural network modeling of creep behavior in a rotating composite disc. Engineering Computations 24(2): 151-164.

Hsu, D.S., Yeh, I.C., Lian, W.T., (1993). Artificial neural damage detection of existing structure, in: Proc. 3rd ROC and Japan Seminar on Natural Hazards Mitigation Conference.

Kalkan, İ., (2010). Deflection prediction for reinforced concrete beams through different effective moment of inertia expressions. International Journal of Engineering Research Development 2(1): 72-80.

Kaloop, M.R., Kim, D.K., (2014). GPS-structural health monitoring of a long span bridge using neural network adaptive filter. Survey Review 16(334): 7-14.

Kanwar, V., Kwatra, N., Aggarwal, P., (2007). Damage detection for framed RCC buildings using ANN modelling. International Journal of Damage Mechanics 16(4): 457-472.

Kim, D.K., Kim, D.H., Cui, J., Seo, H.Y., Lee, Y.H., (2009). Iterative neural network strategy for static model identification of an FRP deck. Steel and Composite Structures 9(5): 445-455.

Maru, S., Nagpal, A.K., (2004). Neural network for creep and shrinkage deflections in reinforced concrete frames.

Journal of Computing in Civil Engineering ASCE 18(4): 350-359.

MATLAB 7.8, (2009). Neural networks toolbox user's guide, USA.

Min, J., Park, S., Yun, C.B., Lee, C.G, Lee, C., (2012). Impedance-based structural health monitoring incorporating neural network technique for identification of damage type and severity. Engineering Structures 39: 210-220.

Mohammadhassani, M., Nezamabadi-Pour, H., Jumaat, M.Z., Jameel, M., Arumugam A.M.S., (2013). Application of artificial neural networks (ANNs) and linear regressions (LR) to predict the deflection of concrete deep beams. Computers and Concrete 11(3): 237-252.

Mohammadhassani, M., Nezamabadi-Pour, H., Jumaat, M.Z., Jameel, M., Hakim, S.J.S., Zargar, M., (2013). Application of the ANFIS model in deflection prediction of concrete deep beam. Structural Engineering and Mechanics 45(3): 319-332.

Patel, K.A., Chaudhary, S., Nagpal, A.K., (2014). Analytical-numerical procedure incorporating cracking in RC beams. Engineering Computations 31(5): 986-1010.

Pendharkar, U., Chaudhary, S., Nagpal, A.K., (2007). Neural network for bending moment in continuous composite beams considering cracking and time effects in concrete. Engineering Structures 29(9): 2069-2079.

Pendharkar, U., Chaudhary, S., Nagpal, A.K., (2010). Neural networks for inelastic mid-span deflections in continuous composite beams. Structural Engineering and Mechanics 36(2): 165-179.

Pendharkar, U., Chaudhary, S., Nagpal, A.K., (2011). Prediction of moments in composite frames considering cracking and time effects using neural network models. Structural Engineering and Mechanics 39(2): 267-285.

Sarkar, K., Gupta, M.K., (2009). Comparative study of optimum design approaches and artificial neural network based optimum design of a singly reinforced concrete beam. Journal of Structural Engineering SERC 36(5): 235-242.

Scanlon, A., Orsak, D.R.C., Buettner, D.R., (2001). ACI code requirements for deflection control: A critical review. ACI Special publications 203-01: 1-14.

Sozen, A., Arcaklioglu, E., Ozalp, M., Kanit, E.G., (2004). Use of artificial neural networks for mapping of solar potential in Turkey. Applied Energy 77: 273-286.

Standards Association of Australia (SAA) AS 3600, (1994). Australian standard for concrete structures, Australia.

Tadesse, Z., Patel, K.A., Chaudhary, S., Nagpal, A.K., (2012). Neural networks for prediction of deflection in composite bridges. Journal of Constructional Steel Research 68(1): 138-149.

Tavakoli, H.R., Omran, O.L., Kutanaei, S.S., Shiade, M.F., (2014). Prediction of energy absorption capability in fiber reinforced self-compacting concrete containing nano-silica particles using artificial neural network. Latin American Journal of Solids and Structures 11(6): 966-979.

Tavakoli, H.R., Omran, O.L., Shiade, M.F., Kutanaei, S.S., (2014). Prediction of combined effects of fibers and nano-silica on the mechanical properties of self-compacting concrete using artificial neural network. Latin American Journal of Solids and Structures 11(11): 1906-1923.

Turkish Standards Institute TS 500, (2000). Requirements for design and construction of reinforced concrete structures, Turkey.

Uddin, M.A., Jameel, M., Razak, H.A., Islam, A.B.M., (2012). Response prediction of offshore floating structure using artificial neural network. Advanced Science Letters 14(1): 186-189.

Washa, G.W., Fluck, P.G., (1952). Effect of compressive reinforcement on the plastic flow of reinforced concrete beams. ACI Journal 49(10): 89-108.

Yu, W.W., Winter, G., (1960). Instantaneous and long-term deflection of reinforced concrete beams under working loads. ACI Journal 57(1): 29-50.